

## Interacting Atomic Interferometry for Rotation Sensing Approaching the Heisenberg Limit

Stephen Ragole<sup>1,2,\*</sup> and Jacob M. Taylor<sup>1,2,3</sup>

<sup>1</sup>*Joint Quantum Institute, University of Maryland, College Park, Maryland 20742, USA*

<sup>2</sup>*Joint Center for Quantum Information and Computer Science, University of Maryland, College Park, Maryland 20742, USA*

<sup>3</sup>*National Institute of Standards and Technology, Gaithersburg, Maryland 20899, USA*

(Received 12 January 2016; published 11 November 2016)

Atom interferometers provide exquisite measurements of the properties of noninertial frames. While atomic interactions are typically detrimental to good sensing, efforts to harness entanglement to improve sensitivity remain tantalizing. Here we explore the role of interactions in an analogy between atomic gyroscopes and SQUIDs, motivated by recent experiments realizing ring-shaped traps for ultracold atoms. We explore the one-dimensional limit of these ring systems with a moving weak barrier, such as that provided by a blue-detuned laser beam. In this limit, we employ Luttinger liquid theory and find an analogy with the superconducting phase-slip qubit, in which the topological charge associated with persistent currents can be put into superposition. In particular, we find that strongly interacting atoms in such a system could be used for precision rotation sensing. We compare the performance of this new sensor to an equivalent noninteracting atom interferometer, and find improvements in sensitivity and bandwidth beyond the atomic shot-noise limit.

DOI: [10.1103/PhysRevLett.117.203002](https://doi.org/10.1103/PhysRevLett.117.203002)

Cold atomic systems have provided an exciting arena for studying aspects of quantum mechanics. The ability to coherently manipulate atoms has been employed to measure the properties of noninertial frames, e.g., Refs. [1,2]. The recent realizations of toroidal traps [3–9] for atoms have presented the possibility for an atomic analogue of the SQUID and its application as a sensor and qubit, e.g., Refs. [10–15]. These systems are well understood when interactions between particles are comparatively weak. However, to achieve the maximum advantages in sensing and other applications, many-body superpositions must be understood and utilized. In this Letter, we propose a method for the reliable creation and manipulation of superpositions of many-body states of cold atoms, in particular, the persistent current states of atoms confined to a 1D ring. As a concrete example, we show how the system sensitivity to rotation can be improved by strong interactions.

Previous approaches to atom interferometric sensing use the ability to transform phase evolution along different paths into population differences, but treat atomic interactions as deleterious to sensitivity [16,17]. In these approaches, e.g., Ramsey interferometry, single atoms are put into superposition and the relative phase gained over some time contains information about the quantity to be measured. The far end of the interferometer converts these phases into measurable population differences. However, atoms can interact during this process, altering the phase and leading to a loss of single atom coherence, decreasing the final sensitivity of the measurement [16,17]. These experiments can be engineered to minimize the possibility

of interaction and they have produced remarkably precise measurements of gravitation and rotation [1,2]. This precision comes in part from conducting a large number of independent single atom measurements simultaneously. These ensemble measurements have a noise-signal ratio limited by the shot noise of  $N$  independent two-level systems. This noise-signal ratio goes as  $1/\sqrt{N}$ , known as the shot noise limit [18]. Sensitivities may be improved even to the limit from Heisenberg uncertainty, but only through atomic entanglement, such as squeezing [19].

This Letter describes a system designed to explore the effect of atomic interactions on the sensitivity of an atomic interferometer to rotational flux. We investigate whether there are situations in which atomic interactions can lead to the correlations necessary to beat the shot noise limit while not being too strongly dephased to prevent sensitivity improvements. We find that a strongly repulsive gas of atoms with a weak barrier can be manipulated to create persistent current state superpositions, which can be used to sense rotation with sensitivity that scales as  $N^{-3/4}$ , below the shot noise limit, but not approaching the Heisenberg limit. Surprisingly, we do not find that SQUID-like systems with strong barriers are effective for this sensing technique. Instead, we utilize the atomic analogue of the phase-slip qubit [20].

Strongly interacting systems are famously challenging to analyze. To reduce the difficulty of this problem, we study only the long wavelength behavior of a gas of atoms trapped in a ring geometry in the 1D limit. This dimensional reduction simplifies the physics involved and allows us to consider a variety of interactions and even statistics,

though we focus on the bosonic case. While current experiments are weakly interacting and, at best, quasi-2D [5–9], 1D linear traps have been achieved with a range of interaction strengths, e.g., Refs. [21,22]. There remains substantial work to create strongly interacting ring systems described above and by others [23–27], but there are efforts in progress [28] and this Letter demonstrates an additional payoff of achieving such systems.

Since we consider a wide range of atomic interactions, perturbative methods are not suitable. Mean-field approximations, such as those underlying the Gross-Pitaevskii equation, miss a crucial quantum effect: the ability to create superpositions of many-body excitations, which we find to be necessary for interaction-assisted metrological benefit. Instead, we employ Luttinger liquid theory, an effective field theory which universally describes quantum systems in one dimension with short-range interactions [29–31].

We require temperatures and time variations that are slow compared to the Luttinger energy scale,  $E_{LL} \approx (\hbar^2 \pi^2 \rho_0^2 / K)$ , where  $\rho_0 = \langle \rho \rangle$  is the average number of atoms per length.  $K$ , the Luttinger parameter, encodes the combined effects of statistics and interactions. For example,  $K = 1$  corresponds to the Tonks-Girardeau gas (or free fermions) and  $K \rightarrow \infty$  is the superfluid limit. The interaction strength of delta function-interacting bosons can be mapped to the Luttinger parameter, which allows us to consider the range of interactions for a repulsive Bose gas [31]. We find that  $K \approx 1$  is ideal for the gyroscope. In this limit, we can express the Luttinger parameter in terms of the 3D scattering length,  $a_s$ , the transverse confinement,  $l_\perp$ , and  $\rho_0$ :  $K = 1 + \{2\rho_0 l_\perp^2 [1 - (Ca_s/l_\perp)] / a_s\}$ , where  $C \approx 1.0325\dots$  is a constant [31]. This theory has the following free Hamiltonian (following conventions from Ref. [31]):

$$H_0 = \frac{\hbar v_s}{2\pi} \int_0^L dx \left( K [\partial_x \phi(x)]^2 + \frac{1}{K} [\partial_x \Theta(x) - \pi \rho_0]^2 \right), \quad (1)$$

where  $v_s$  is the speed of sound,  $L$  is the circumference of the ring,  $\phi(x)$  is a local phase of the underlying field which we are abstracting away.  $\partial_x \Theta(x)$  relates to the number density,  $\rho$ , by  $\rho(x) = [\partial_x \Theta(x) / \pi] \sum_{l=-\infty}^{+\infty} e^{2il\Theta(x)}$ . The Luttinger fields  $\phi(x)$  and  $\Theta(x)$  have the following commutation relation,  $[\phi(x), \partial_{x'} \Theta(x') / \pi] = i\delta(x - x')$ .

To make the system sensitive to rotation, we break rotational symmetry by adding a blue-detuned laser beam as a localized potential barrier, shown in Fig. 1. We approximate the laser in the long wavelength theory as a (moving) barrier at a single point ( $x = x_b(t)$ ) on the ring. When the barrier is smaller than  $E_{LL}$ , i.e., weak, it induces a new term in the Hamiltonian [30–33]:

$$V = \int_0^L dx U_0 \delta(x - x_b(t)) \rho(x) \approx 2NU_0 \cos\{2\Theta(x_b(t))\}, \quad (2)$$

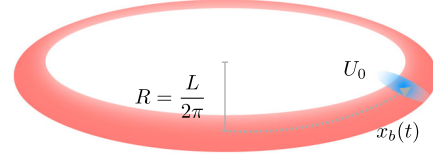


FIG. 1. A cartoon of the system. Atoms are trapped in a 1D ring of length  $L$  with a blue-detuned laser crossing at a single point,  $x_b(t)$ . In the atom frame, the barrier rotates through the ring at a rate combining the laboratory frame rotation [ $\omega_{\text{frame}} = (2\pi v_{\text{frame}}/L)$ ] and the externally controlled stirring rate [ $\omega_{\text{stir}} = (2\pi v_{\text{stir}}/L)$ ].

where  $N$  is the particle number, and  $U_0$  is the dipole potential from the laser. In this expansion, we have kept the lowest harmonics of the density (consistent with Refs. [30,32,33]). Though strong laser barriers have been used to create “weak links,” in one dimension such barriers will destroy persistent current states. The weak barrier considered here preserves the character of persistent current states and couples them perturbatively.

We perform a standard field expansion for periodic boundary conditions [31,34]. This expansion defines the fields in terms of zero modes ( $\theta_0, \phi_0$ ), topological excitations ( $N, J$ ), and phonons ( $b_q$ ). Explicitly,

$$\Theta(x) = \theta_0 + \frac{\pi x}{L} N + \frac{1}{2} \sum_{q \neq 0} \left| \frac{2\pi K}{qL} \right|^{\frac{1}{2}} (e^{iqx} b_q + e^{-iqx} b_q^\dagger), \quad (3)$$

$$\phi(x) = \phi_0 + \frac{2\pi x}{L} J + \frac{1}{2} \sum_{q \neq 0} \left| \frac{2\pi}{qLK} \right|^{\frac{1}{2}} \text{sgn}(q) (e^{iqx} b_q + e^{-iqx} b_q^\dagger). \quad (4)$$

In this expansion,

$$H_0 = \sum_{q \neq 0} \hbar \omega(q) b_q^\dagger b_q + \frac{\rho_0 L \hbar \omega_0}{8K^2} (N - \rho_0 L)^2 + \frac{\rho_0 L \hbar \omega_0}{2} J^2, \quad (5)$$

where  $\omega_0 = (4\pi^2 \hbar / ML^2)$  is the rotation quantum for particles of mass  $M$  in a ring of circumference  $L$  and we use the relation  $v_s K = (\hbar \pi N / ML)$  from Galilean invariance to achieve this form. We restrict our consideration to a fixed atom number ( $N = \rho_0 L$ ). The current operator  $J$  has integer eigenvalues and represents the topological charge associated with persistent current in the ring. The phonon modes,  $b_q$ , are bosons with quasimomentum  $q_n = (2\pi n / L)$  for  $n \in \mathbb{Z}$  and  $\omega(q) = \hbar v_s |q|$  for  $q \ll \rho_0$ .

Now, we transform to a frame which is corotating with the barrier. The barrier rotates along with the lab frame and can be actively controlled relative to the lab frame to “stir” the gas. Noting  $[J, 2\theta_0] = i$  and  $[b_q, b_{q'}^\dagger] = \delta_{qq'}$ , we transform the Hamiltonian with  $U_{\text{rf}} = \exp[-i(\{[2\pi x_b(t)N]/L\}J + \sum_{q \neq 0} q x_b(t) b_q^\dagger b_q)]$ .

The free Hamiltonian is invariant under the transformation, while  $V \rightarrow 2NU_0 \cos[2\Theta(0)]$ . We also gain the terms

$$\delta H = -i\hbar U_{\text{eff}}^\dagger \dot{U}_{\text{eff}} = -\hbar \omega_b(t) NJ - \hbar \sum_{q \neq 0} q \dot{x}_b(t) b_q^\dagger b_q, \quad (6)$$

where  $\omega_b(t) = [2\pi \dot{x}_b(t)/L]$  is the angular frequency of the barrier relative to the atoms.

We complete the square for the linear  $J$  term and ignore the constant term produced under our fixed atom number assumption. Thus, the transformation leads to a shift in the persistent current operator  $J^2 \rightarrow \{J - [\omega_b(t)/\omega_0]\}^2$ . The phonon term is easily absorbed by defining a new phonon dispersion relation,  $\tilde{\omega}(q) = v_s |q| - \dot{x}_b(t)q$ . This shifted frequency confirms the intuition that if the stirring speed  $\dot{x}_b$  grows larger than the sound velocity  $v_s$  our theory will become unstable.

Adding in a barrier breaks the Galilean invariance, and can couple phonons and topological excitations to themselves and each other, potentially decohering topological charge superpositions. We can expand the barrier term using Eq. (3),

$$V = NU_0 (e^{2i[\theta_0 + \delta\theta(0)]} + e^{-2i[\theta_0 + \delta\theta(0)]}), \quad (7)$$

where  $\delta\theta(0) = \frac{1}{2} \sum_{q \neq 0} |2\pi K/qL|^{1/2} (b_q + b_q^\dagger)$  is the phonon contribution to the field.

We focus on the coupling of topological charge states, which are most suited for sensing applications. Thus, we integrate over the phonon modes to determine the effective interaction between the persistent current states. Following Refs. [32–34], we arrive at the following expression for the potential barrier.

$$\begin{aligned} V &= NU_0 e^{2i\theta_0} \langle e^{2i\delta\theta(0)} \rangle_{\delta\theta} + \text{H.c.} \\ &= 2NU_{\text{eff}} \cos(2\theta_0), \end{aligned} \quad (8)$$

where the brackets denote functional integration over the phonon modes,  $U_{\text{eff}} = U_0 (d/L)^K$  is the renormalized barrier strength, and  $d$  is a short distance cutoff. While Luttinger liquid theory has a cutoff above which it loses validity [ $E_{\text{LL}} \approx (N^2 \hbar \omega_0 / 4K)$ ], this renormalization step gives a lower cutoff,  $E_{\text{ph}} = (N \hbar \omega_0 / 4K) \approx (E_{\text{LL}} / N)$ . The new cutoff generates a time scale below which the renormalized theory is not valid, which will be important to consider when manipulating the system. Simply put, working below the lowest phonon mode frequency prevents decoherence but lowers the “max velocity” for diabatic processes.

The barrier renormalization depends on both the microscopic details and the Luttinger parameter,  $K$ . Here we see the first nontrivial indication of the interactions: in the superfluid limit ( $K \rightarrow \infty$ ), a barrier will be weakened significantly by the phononic modes. However, in the

strongly repulsive ( $K \rightarrow 1$ ) regime, the barrier will remain finite, allowing mixing between current states. The relevant cutoff for this regime is  $d \approx (KL/N)$ , so  $U_{\text{eff}} = U_0 (K/N)^K$  [34]. In this limit, the strongest constraint on the barrier is that it must be weak,  $2NU_0 < (N^2 \hbar \omega_0 / 4K)$ . This restriction guarantees that the perturbative and adiabatic constraints will be satisfied, since after renormalization  $2NU_{\text{eff}} = 2N^{1-K} U_0 K^K < (N^{2-K} \hbar \omega_0 / 4K^{1-K}) < E_{\text{ph}}$ . Fixing the weakness of the barrier sets  $U_0 = U_{\text{weak}} N$ , where  $U_{\text{weak}} < (\hbar \omega_0 / 8K)$ .

This Hamiltonian, similar to the quantum phase-slip junction [20], is the dual of the standard superconducting charge qubit Hamiltonian [35]:

$$H_{JJ} = E_c (n - n_g)^2 - E_J \cos(\delta), \quad (9)$$

where  $n$  is the number of Cooper pairs on the island,  $n_g$  is set by the gate voltage,  $\delta$  is the phase difference across the junction, and  $[\delta, n] = i$ . Under the substitution  $n \rightarrow J$  and  $\delta \rightarrow -2\theta_0$ , the current states form a charge-qubit-like system with  $E_C = (N \hbar \omega_0 / 2)$  and  $E_J = 2N^{1-K} U_0 K^K$  ( $E_J \ll E_C$ , since the barrier is perturbative).

Since the barrier couples the current state  $|J\rangle$  to states  $|J'\rangle = |J \pm 1\rangle$ , superpositions can be formed by precisely controlling the rotation rate of the stirring beam. Consider preparing the atoms without any rotation,  $|\Psi\rangle = |0\rangle$ . Here, only the states  $|\pm 1\rangle$  will be coupled by the barrier and only mix weakly into the ground state at  $\omega = 0$ . We can implement a  $\pi/2$  pulse in the two steps illustrated in Fig. 2(a). First, we adiabatically increase rotation to  $\omega = (\omega_0/2)$ , where the instantaneous ground state is  $(1/\sqrt{2})(|0\rangle - |1\rangle)$ . Then, the rotation rate is diabatically ramped back to  $\omega = 0$  and the barrier turned off. This process will be completed in a time  $\tau_{\pi/2} = \tau_{\text{adiabatic}} + \tau_{\text{diabatic}}$ . These times can be determined from a Landau-Zener analysis of the effective two-level system and will be set by the effective barrier height,  $\tau_{\pi/2} \propto (\hbar / NU_{\text{eff}})$ .

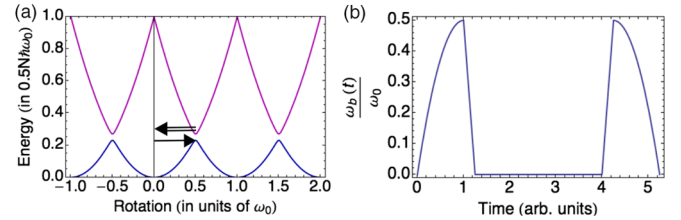


FIG. 2. (a) The energy spectrum for the perturbed current states, lower (upper) represents the ground (excited) state. The weak barrier creates avoided crossings at rotation  $\omega = (n + 1/2)\omega_0$ ,  $n \in \mathbb{Z}$ . The arrows represent the proposed “ $\pi/2$  pulse”: the system is adiabatically driven to the avoided crossing (single arrow) and diabatically returned  $\omega = 0$  (double arrow). (b) A cartoon of the proposed Ramsey sequence. The sequence consists of two  $\pi/2$  pulses with an observation time  $\tau_{\text{obs}}$  in between.

Having established the charge-qubit-like behavior and appropriate sequences for preparing topological charge superpositions, we now propose a Ramsey interferometry scheme for rotation sensing, using the persistent current states as the basis. As described above, we create a superposition of current states,  $(1/\sqrt{2})(|0\rangle - |1\rangle)$ , and turn the barrier off. Then, we expose this superposition to a small rotation rate ( $\omega \ll \omega_0$ ) for a time  $\tau_{\text{obs}}$  without the barrier. Over this time, the superposition will evolve into the state  $(1/\sqrt{2})(|0\rangle - e^{i\phi}|1\rangle)$ , where  $\phi = N\tau_{\text{obs}}[(\omega_0/2) - \omega]$ . This phase can be converted into a population difference by performing another  $\pi/2$  pulse. A cartoon of the process is pictured in Fig. 2(b). The final state can be read-out from the persistence of a vortex core in time-of-flight imaging. If the state projects to  $|1\rangle$ , the vortex will be visible as an absence of density in the center of the ring, while  $|0\rangle$  will expand isotropically, filling the central core [6]. As the relative phase between many-body excitations, the phase scales with the number of atoms while the vortex shot noise is constant. Therefore, the nominal sensitivity to rotation has Heisenberg-like scaling in the absence of noise.

The proposed gyroscope is most viable in the strongly interacting limit which maintains the gap needed to couple persistent current states and keeps  $\tau_{\pi/2}$  short. While our analysis has only considered a clean system, it is likely that there will be disorder present in the trap. Disorder leads to localization in one dimension for  $K < 1.5$  [30]. Therefore, the optimal  $K$  is just above this localization limit. While this limit is acceptable for simple experiments, a more detailed analysis of trap imperfections will be necessary for improving future experiments.

We consider realistic sources of noise that could affect the sensitivity. In particular, we will consider shot-to-shot variation in the atom number. Other systematic noise issues, such as laser power and trap configuration fluctuations, could be problematic but can be surmounted with sufficient detuning and laser power.

To compute the effect of shot-to-shot variations in atom number, we assume that number fluctuations are Poissonian,  $\sigma_N = \sqrt{N}$ . We can consider each individual run of the experiment as having some fixed signal and a random additional noise. We define  $F = (\omega_0/2) - \omega$  and  $\delta N_i$  as the noise in the atom number. We consider an average of many measurements over the noise:

$$\begin{aligned} \langle e^{i\phi} \rangle &= \langle e^{i(NF\tau_{\text{obs}} + \delta N_i F \tau_{\text{obs}})} \rangle \\ &\approx e^{iNF\tau_{\text{obs}}} e^{-F^2 \sigma_N^2 \tau_{\text{obs}}^2} \end{aligned} \quad (10)$$

While in the absence of noise, longer evolution times would produce higher sensitivity, the low frequency noise decreases contrast as  $e^{-F^2 \sigma_N^2 \tau_{\text{obs}}^2}$  as  $\tau_{\text{obs}}$  increases. With this noise added in, we can calculate the sensitivity of our approach:

$$\begin{aligned} S &= \left| \partial_\omega \frac{\text{Signal}}{\text{Noise}} \right|_{\omega=0}^{-1} \sqrt{\tau_{\text{obs}}} \\ &= \left| \frac{N\omega_0\tau_{\text{obs}} \sin(NF_0\tau_{\text{obs}} + \phi_0) e^{-F_0^2 \sigma_N^2 \tau_{\text{obs}}^2}}{2F_0} \right|^{-1} \sqrt{\tau_{\text{obs}}} \\ &= \frac{e^{(\omega_0^2/4)\sigma_N^2 \tau_{\text{obs}}^2}}{N\sqrt{\tau_{\text{obs}}}}, \end{aligned} \quad (11)$$

where in the last line, we have used  $F_0 = F(\omega = 0) = (\omega_0/2)$ . We can optimize  $\tau_{\text{obs}}$  and determine the best sensitivity for the device. Using the optimum observation time,  $\tau_{\text{obs}}^* = (1/\omega_0\sigma_N)$ , we calculate,  $S_{\text{max}} = (e^{1/4} \sqrt{\omega_0\sigma_N}/N)$ .

We see that a Poisson-distributed number of atoms per “shot” changes the ideal Heisenberg-like scaling for  $N$  fixed to  $N^{-3/4}$  scaling. However, this is still an improvement over the shot-noise limit. It could be further enhanced if the time-of-flight images from vortex detection are calibrated to give a sub-Poissonian estimate of atom number, effectively reducing  $\sigma_N$ .

Using a gas temperature of 100 nK and ring radius  $R = 19.2 \mu\text{m}$  [5–7], we assume a transverse confinement of  $l_\perp \approx 200 \text{ nm}$ , which gives  $a_s \approx 3600a_0$ , where  $a_0$  is the Bohr radius, to set  $K \approx 1.6$  for  $N = 10^5$ . Estimating  $\sigma_N = (\sqrt{N}/10)$ , we find that a sensor with  $N = 10^5$  atoms would have  $\tau_{\pi/2} = 0.8 \text{ s}$ ,  $\tau_{\text{obs}}^* \approx 4 \text{ ms}$ , a sensitivity of  $2 \times 10^{-4} (\text{rad}/\text{s}\sqrt{\text{Hz}})$  and a bandwidth  $\geq 200 \text{ Hz}$ . Since the entanglement allows relatively rapid phase accumulation, the sensor has a higher bandwidth than noninteracting sensors. To reasonably compare these techniques, we instead consider a sensitivity per root bandwidth.

We plot the numerical results for optimum sensitivity as a function of atom number  $N$  and compare with the noiseless limit and an equal area atom interferometer as described in Ref. [1], each evaluated for a fixed time  $\tau_{\text{comp}} = (2\pi/\omega_0) = 0.838 \text{ s}$  in Fig. 3. This time is set by the circumnavigation time for atoms moving at the persistent current velocity and is much longer than optimal observation for the Luttinger system,  $\tau_{\text{comp}} \approx 6 \times \max(\tau_{\text{obs}}^*)$ . In the atom interferometer, the atoms will gain a Sagnac phase of  $\phi = (2M/\hbar)\omega A$ ,

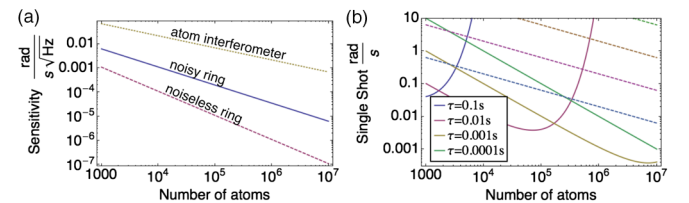


FIG. 3. (a) The sensitivity of our proposed gyroscope (solid) plotted on a log-log scale as a function of atom number. The dashed (dotted) line represents the sensitivity for a noiseless Luttinger (atom interferometer) system with an observation time of  $\tau_{\text{comp}} = 0.838 \text{ s}$ . (b) Solid (dashed) lines: The single-shot sensitivity for the noisy Luttinger (atom interferometer) system for different observation times,  $\tau$ , as a function of atom number.

where  $A = (L^2/4\pi)$  is the area enclosed by the atoms. This phase can be conveniently rewritten,  $\phi = (2\pi MR^2/\hbar)\omega = \omega\tau_{\text{comp}}$ . The sensitivity for the comparison noninteracting system will be

$$S_{SA} = \frac{1}{|\partial_\omega [\frac{1}{2} \cos(\omega\tau_{\text{comp}} + \phi_0)]|} \sqrt{\frac{\tau_{\text{comp}}}{N}},$$

$$S_{SA_{\text{max}}} = \frac{2}{\sqrt{N\tau_{\text{comp}}}}. \quad (12)$$

The sensitivity is improved in the Luttinger ring system, Fig. 3(a). The noninteracting atomic case shows scaling  $\propto N^{-1/2}$  due to the shot-noise limit. Similarly, the noiseless Luttinger system shows Heisenberg-like scaling ( $\propto N^{-1}$ ) while the noisy case sits in between. The single shot sensitivity, Fig. 3(b), demonstrates the trade-offs between longer observation times and atom number.

We note that preparing the Luttinger system takes much longer than the observation time. In our example case,  $\tau_{\text{prep}} \approx 0.8$  s for the  $(\pi/2)$  pulse; so too does  $\tau_{\text{measure}} \approx \tau_{\text{prep}}$ , which results in a long time between measurements. Faster preparation techniques would substantially improve performance. In addition, atom interferometers can achieve sensitivities much lower than those presented here by using many more atoms and a large enclosed area as shown in Ref. [1].

While the system shows limited application for high sensitivity rotational sensing, the size of the system makes it a compelling candidate for inertial tests, such as inverse-square law tests, where short length scales are difficult to probe [36–38]. In particular, several high-energy theories predict deviations from Newtonian gravity at the micron scale [36,39–41]. The ring system described above shows promise in detecting these deviations. However, designing and optimizing such a test will require further research and is beyond the scope of this Letter.

A detailed analysis of the limitations on coherent superpositions in Luttinger liquids will be needed for a complete understanding of this type of gyroscope. Though we controlled the dominant dephasing mechanism by working slowly enough to avoid creating phonons, it is not obvious how stable the superposition will be if particle loss is included. Simulations of superpositions of atoms ( $N < 10$ ) suggest that the strongly repulsive regime considered here ( $K \rightarrow 1$ ) may be robust to particle loss but it is unclear if these results extend to many atoms [25]. Still, the scheme allows the creation of a many-body superposition with sensitivity to small rotation rates and shows favorable scaling, even in the presence of noise. In addition to rotation or inertial sensing, it is possible that creating these superpositions will have other interesting applications, e.g., for use as qubits [26,27,42].

We thank L. Mathey, G. K. Campbell, and G. Zhu for insightful discussions and helpful feedback. Funding was provided by the NSF supported Physics Frontier Center (Grant No. PHYS 1430094) at the JQI.

\*ragole@umd.edu

- [1] T. L. Gustavson, P. Bouyer, and M. A. Kasevich, *Phys. Rev. Lett.* **78**, 2046 (1997).
- [2] M. J. Snadden, J. M. McGuirk, P. Bouyer, K. G. Haritos, and M. A. Kasevich, *Phys. Rev. Lett.* **81**, 971 (1998).
- [3] S. Gupta, K. W. Murch, K. L. Moore, T. P. Purdy, and D. M. Stamper-Kurn, *Phys. Rev. Lett.* **95**, 143201 (2005).
- [4] C. Ryu, M. F. Andersen, P. Cladé, V. Natarajan, K. Helmerson, and W. D. Phillips, *Phys. Rev. Lett.* **99**, 260401 (2007).
- [5] A. Ramanathan, K. C. Wright, S. R. Muniz, M. Zelan, W. T. Hill, C. J. Lobb, K. Helmerson, W. D. Phillips, and G. K. Campbell, *Phys. Rev. Lett.* **106**, 130401 (2011).
- [6] K. C. Wright, R. B. Blakestad, C. J. Lobb, W. D. Phillips, and G. K. Campbell, *Phys. Rev. Lett.* **110**, 025302 (2013).
- [7] S. Eckel, J. G. Lee, F. Jendrzejewski, N. Murray, C. W. Clark, C. J. Lobb, W. D. Phillips, M. Edwards, and G. K. Campbell, *Nature (London)* **506**, 200 (2014).
- [8] S. Moulder, S. Beattie, R. P. Smith, N. Tammuz, and Z. Hadzibabic, *Phys. Rev. A* **86**, 013629 (2012).
- [9] C. Ryu, P. Blackburn, A. A. Blinova, and M. Boshier, *Phys. Rev. Lett.* **111**, 205301 (2013).
- [10] T. P. Orlando, S. Lloyd, L. S. Levitov, K. K. Berggren, M. J. Feldman, M. F. Bocko, J. E. Mooij, C. J. P. Harmans, and C. H. Van Der Wal, *Physica (Amsterdam)* **372C–376C**, 194 (2002).
- [11] J. R. Friedman, J. R. Friedman, V. Patel, V. Patel, W. Chen, W. Chen, S. Tolpygo, S. Tolpygo, J. E. Lukens, and J. E. Lukens, *Nature (London)* **406**, 43 (2000).
- [12] F. Wellstood, C. Heiden, and J. Clarke, *Rev. Sci. Instrum.* **55**, 952 (1984).
- [13] B. Yurke, P. G. Kaminsky, R. E. Miller, E. A. Whittaker, A. D. Smith, A. H. Silver, and R. W. Simon, *Phys. Rev. Lett.* **60**, 764 (1988).
- [14] I. Siddiqi, R. Vijay, F. Pierre, C. M. Wilson, M. Metcalfe, C. Rigetti, L. Frunzio, and M. H. Devoret, *Phys. Rev. Lett.* **93**, 207002 (2004).
- [15] J. Clarke and A. I. Braginski, *The SQUID Handbook Fundamentals and Technology of SQUIDS and SQUID Systems* (Wiley-VCH, Weinheim, 2006), Vol. 1.
- [16] S. Dimopoulos, P. W. Graham, J. M. Hogan, and M. A. Kasevich, *Phys. Rev. D* **78**, 042003 (2008).
- [17] R. Jannin, P. Cladé, and S. Guellati-Khélifa, *Phys. Rev. A* **92**, 013616 (2015).
- [18] C. M. Caves, K. S. Thorne, R. W. P. Drever, V. D. Sandberg, and M. Zimmermann, *Rev. Mod. Phys.* **52**, 341 (1980).
- [19] V. Giovannetti, S. Lloyd, and L. Maccone, *Science* **306**, 1330 (2004).
- [20] J. E. Mooij and Y. V. Nazarov, *Nat. Phys.* **2**, 169 (2006).
- [21] T. Kinoshita, T. Wenger, and D. S. Weiss, *Science* **305**, 1125 (2004).
- [22] F. Meinert, M. Panfil, M. J. Mark, K. Lauber, J. S. Caux, and H. C. Nägerl, *Phys. Rev. Lett.* **115**, 085301 (2015).
- [23] R. Citro, A. Minguzzi, and F. W. J. Hekking, *Phys. Rev. B* **79**, 172505 (2009).
- [24] N. Didier, A. Minguzzi, and F. W. J. Hekking, *Phys. Rev. A* **79**, 063633 (2009).
- [25] D. W. Hallwood, T. Ernst, and J. Brand, *Phys. Rev. A* **82**, 063623 (2010).

- [26] D. Solenov and D. Mozysrsky, *Phys. Rev. Lett.* **104**, 150405 (2010).
- [27] D. Solenov and D. Mozysrsky, *Phys. Rev. A* **82**, 061601(R) (2010).
- [28] Y. Cai and K. C. Wright (private communication).
- [29] F. Haldane, *Phys. Rev. Lett.* **47**, 1840 (1981).
- [30] T. Giamarchi, *Quantum Physics in One Dimension*, Int. Series of Monographs on Physics (Clarendon Press, New York, 2003).
- [31] M. A. Cazalilla, *J. Phys. B* **37**, S1 (2004).
- [32] C. L. Kane and M. P. A. Fisher, *Phys. Rev. Lett.* **68**, 1220 (1992).
- [33] C. L. Kane and M. P. A. Fisher, *Phys. Rev. B* **46**, 15233 (1992).
- [34] M. Cominotti, D. Rossini, M. Rizzi, F. Hekking, and A. Minguzzi, *Phys. Rev. Lett.* **113**, 025301 (2014).
- [35] A. Shnirman, G. Schön, and Z. Hermon, *Phys. Rev. Lett.* **79**, 2371 (1997).
- [36] E. G. Adelberger, B. R. Heckel, and A. E. Nelson, *Annu. Rev. Nucl. Part. Sci.* **53**, 77 (2003).
- [37] J. H. Gundlach, *New J. Phys.* **7**, 205 (2005).
- [38] D. J. Kapner, T. S. Cook, E. G. Adelberger, J. H. Gundlach, B. R. Heckel, C. D. Hoyle, and H. E. Swanson, *Phys. Rev. Lett.* **98**, 021101 (2007).
- [39] D. B. Kaplan and M. B. Wise, *J. High Energy Phys.* **08** (2000) 037.
- [40] R. Sundrum, *Phys. Rev. D* **69**, 044014 (2004).
- [41] N. Arkani-Hamed, S. Dimopoulos, and G. Dvali, *Phys. Rev. D* **59**, 086004 (1999).
- [42] D. Aghamalyan, M. Cominotti, M. Rizzi, D. Rossini, F. Hekking, A. Minguzzi, L.-C. Kwek, and L. Amico, *New J. Phys.* **17**, 045023 (2015).